Preliminary results on TeV sources search with AGILE

A. Rappoldi [a,*], F. Longo [b,c], A. Argan [d], G. Barbiellini [b,c], F. Boffelli [a], A. Bulgarelli [e], P. Caraveo [f], P.W. Cattaneo [a], A.W. Chen [f,g], V. Cocco [d], S. Colafrancesco [k], E. Costa [d], F. D' Ammando [d,i], G. De Paris [d], E. Del Monte [d], G. Di Cocco [e], I. Donnarumma [d], Y. Evangelista [d], A. Ferrari [g,h], M. Feroci [d], M. Fiorini [f], T. Froysland [i,g], F. Fuschino [e], M. Galli [j], F. Gianotti [e], P. Giommi [k], A. Giuliani [f], C. Labanti [e], I. Lapshov [d], F. Lazzarotto [d], P. Lipari [l], M. Marisaldi [e], M. Mastropietro [m], S. Mereghetti [f], E. Morelli [e], E. Moretti [b,c], A. Morselli [a], L. Pacciani [d], A. Pellizzoni [o], F. Perotti [f], G. Piano [d,i,n], P. Picozza [i,n], M. Pilia [p], C. Pittori [k], G. Porrovecchio [d], M. Prest [q], G. Pucella [r], M. Rapisarda [r], A. Rubini [d], S. Sabatini [d,i], L. Salotti [s], P. Santolamazza [k], P. Soffitta [d], E. Striani [i,n], M. Tavani [d,i], M. Trifoglio [e], A. Trois [d], E. Vallazza [b], F. Verrecchia [k], S. Vercellone [t], V. Vittorini [d,i], A. Zambra [f], D. Zanello [l]

[a] INFN Pavia, I-27100 Pavia, Italy
[b] INFN Trieste, Padriciano 99, I-34012 Trieste, Italy
[c] Dip. Fisica Università di Trieste, I-34127 Trieste, Italy
[d] INAF/IASF-Roma, I-00133 Roma, Italy
[e] INAF/IASF-Bologna, I-40129 Bologna, Italy
[f] INAF/IASF-Milano, I-20133 Milano, Italy
[g] CIFS-Torino, I-10133 Torino, Italy
[h] Dip. Fisica, Universitá di Torino, Turin, Italy
[i] Dip. di Fisica, Univ. Tor Vergata, I-00133 Roma, Italy
[j] ENEA-Bologna, I-40129 Bologna, Italy
[k] ASI Science Data Center, I-00044 Frascati (Roma), Italy
[l] INFN Roma La Sapienza, I-00185 Roma, Italy
[m] CNR-IMIP, Roma, Italy
[n] INFN Roma Tor Vergata, I-00133 Roma, Italy
[o] INAF-Osservatorio Astronomico di Cagliari, Poggio dei Pini, I-09012 Capoterra, Italy
[p] Dipartimento di Fisica, Università dell'Insubria, I-22100 Como, Italy
[q] Dip. di Fisica, Univ. Dell'Insubria, I-22100 Como, Italy
[r] ENEA Frascati, I-00044 Frascati (Roma), Italy
[s] Agenzia Spaziale Italiana, I-00198 Roma, Italy
[t] INAF-IASF Palermo, I-90146 Palermo, Italy

ARTICLE INFO

ABSTRACT

During its first 2 years of operation, the gamma-ray AGILE satellite almost completed a full study of the gamma-ray sky. This paper presents the preliminary results of the systematic study performed on the AGILE data to search for GeV counterparts and to derive flux upper limits of the TeV sources detected by various instruments (MAGIC, HESS, VERITAS, Cangaroo, MILAGRO, ARGO,….).

© 2010 Elsevier B.V. All rights reserved.

1. Introduction

The space program AGILE (*Astro-rivelatore Gamma a Immagini Leggero*) is a high-energy astrophysics mission [1] supported by the Italian Space Agency (ASI) with scientific and programmatic participation of INAF, INFN, several Italian universities and other research institutions.

The AGILE satellite was successfully launched on 2007 April 23 from the Indian base of Sriharikota. The AGILE instrument is made of three detectors—surrounded by an anticoincidence system [2]—with broad-band detection and imaging capabilities:

- The *Gamma-Ray Imaging Detector* (GRID) is sensitive in the energy range 30 MeV–50 GeV and consists of a silicon–tungsten tracker, a CsI calorimeter, and an anticoincidence system. The GRID is designed to achieve an optimal angular resolution (source location $\sim 0.25°$ for intense sources) and an unprecedentedly large FOV (~ 2.5 sr) [3].

- The *hard X-ray imager* (SuperAGILE) is a coded mask imager placed on the top of gamma-ray detector and sensitive in the energy range 18–60 keV, with an optimal angular resolution (6 arcmin) and a FOV of about 1 sr [4].
- The *Mini-Calorimeter* (MCAL) is part of the GRID, but it is also capable of independently detecting GRBs and other transients in the 350 keV–100 MeV energy range with optimal timing capability [5].

The data collected by AGILE GRID during the first two years of operation of the satellite has been automatically analysed with the aim of measuring or giving an estimate of the GeV flux of the known TeV gamma-sources detected by other experiments, in different time periods, giving the opportunity to search or to identify the correspondent counterparts also in High Energy.

2. TeV sources in the TeVCat

The analysis presented in this paper has been accomplished selecting the sources described into the web-based catalog *TeVCat* [6]. At present, the catalog contains a total of 110 TeV sources; 75 of those—shown in Fig. 1—are classified as *Default Catalog* and are published on refereed journals.

These sources have been considered in our analysis. We decided to use the *TeVCat*, since it is constantly updated with the new TeV sources being detected and published by the various Observatories. *TeVCat* lists also the basic properties of the various sources (location, type, distance, possible association, discoverer, ...). Currently some source classes have been clearly identified, such as extragalactic objects (Blazars and Radio Galaxies), Supernovae Remnants, Pulsar Wind Nebulae, Very High Energy Sources, Gamma-ray Binaries, and Dark Sources [7]. Our analysis is currently being performed for both extragalactic and galactic sources in a systematic way as described below. Moreover detailed source morphology studies will be developed on some specific targets.

3. Data analysis procedure

The whole sample of AGILE GRID data are grouped in *Observation Blocks* (OB), each of which corresponds to a different *pointing* of the satellite in the sky (defined by the galactic coordinates l and b) and may have a different duration (ranging from one day to ~ 30 days). Among them, a set of 79 OBs, covering the period from 2007 May 24 to 2009 April 15, with a total observation duration of 690 day, has been analysed.

Due to the main goals of the AGILE mission, the satellite was principally pointed to observe the two regions of the galactic plane around to $l = 90°$ and $270°$, as shown in the exposure map of

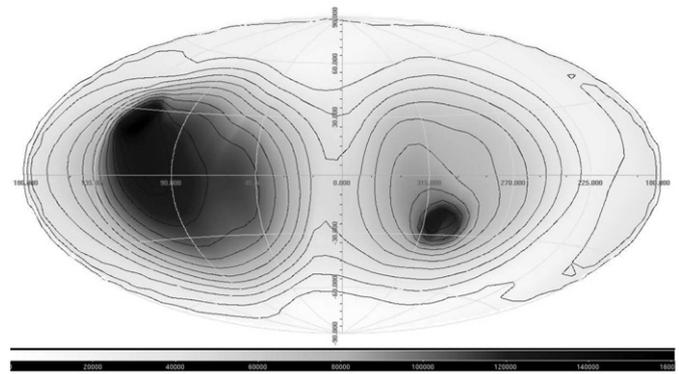**Fig. 2.** Total AGILE GRID exposure map accumulated in about two years of operation. The exposure values are expressed in cm^2.

Fig. 2. Clearly, this characteristic is not optimal for the TeV sources detection—especially for what concern the extragalactic sources—as can be seen comparing the AGILE GRID exposure map with the TeV sources distribution shown in Fig. 1.

An automatic procedure has been created and executed in order to select all the possible known TeV sources that may give some meaningful results with the AGILE data, adopting the following criteria.

Within each pointing, only the TeV sources located at an off-axis angle lower than $40°$ (with respect to the GRID axis, i.e. the pointing center) are considered, to grant the best event selection and accuracy in the γ−ray reconstruction. Under these conditions, 73 sources over 75 of the TeVCat catalog (53 on the galactic plane, 20 extragalactic) result to have useful exposition, giving a total of 773 *observation slots* (608 galactic and 165 extragalactic), defined as a delimited region of the sky centered on the selected TeV source, observed during a given OB. For each *observation slot* the relevant maps (counts, exposure and galactic diffuse background) are generated, with the two different energy threshold $E_\gamma \geq 100$ and 400 MeV.

All these maps are centered on the selected TeV source position, and have the size of $15° \times 15°$, divided into 101×101 bins of $0.15° \times 0.15°$ each one.

The count maps are generated using the *event filter* named FT3ab, that is characterized by a very good track reconstruction and event selection up to angle of $\sim 50°$ with respect to the GRID pointing axis, allowing a high confidence analysis of the selected TeV sources.

The source detection is accomplished by means of a *multi-source* likelihood algorithm, fixing the position of the source on its known coordinates (as given bt TeVCat catalog) and taking into account the position and the flux of all the other known γ−sources situated within a radius of $10°$ from the analysed TeV source, as listed on the EGRET [8], AGILE [9] and FERMI [10] catalogs. When a known source is listed in more than one of such catalogs, the position and the flux of the correspondent source with the best accuracy is taken.

The detection algorithm returns the ratio between the likelihood L_0 of the null hypothesis (diffuse background only) and the likelihood L_1 of the alternative hypothesis (presence of a point-like source). More precisely, using the *Test Statistic* (TS) defined, according to the Wilks' theorem [11], as

$$TS = -2\log(L_0 - L_1)$$

the significance of a source detection with number of counts N large enough ($N \geq 20$) is given by a standard deviation σ equal to $\sqrt{TS}$.

The maximum likelihood algorithm gives the computed value of the flux for the detected source; if $TS > 3$ it represents the
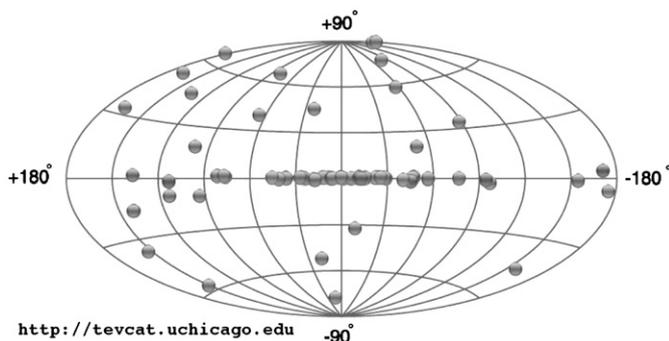

Fig. 1. Simplified map of the 75 TeV sources described in the TeVCat "*Default Catalog*". About $\frac{1}{4}$ of the sources are locate far from the galactic plane.

estimated flux of the TeV source into the selected energy range, otherwise it has to be interpreted as an upper limit at a confidence level of 95%.

4. Results

Applying the described analysis procedure on the whole data set described in the previous section, the flux values (or the flux upper limits) are computed for many TeV sources during the different OBs.

In particular, using the energy threshold $E_\gamma \geq 100$ MeV, the flux can be estimated for 73 TeV sources, whereas the flux is computed for 69 TeV sources when the energy threshold $E_\gamma \geq 400$ MeV is considered.

For several TeV sources the flux value is available for many different OB, allowing to determine the corresponding *light curve*.

In the following only few cases will be shown as meaningful examples of the obtained results.

4.1. Crab

The TeVCat catalog reports the TeV source named TeV J0534+220, identified as the Crab pulsar located at $l = 184.56°$, $b = -5.78°$. This source was used as a calibration source at the beginning of the AGILE satellite operation time both for the GRID and SuperAGILE, and hence it is well visible in many OBs.

Fig. 3 shows the count map, centered on the Crab coordinates, obtained with the data of the OB starting at 2008-08-31 12:00 (UT) and ending at 2008-09-10 12:00 (UT), with an energy threshold $E_\gamma \geq 100$ MeV.

The position of the source TeV J0534+220 corresponds to that of the known gamma sources 0FGL J0534.6+2201, 1AGL J0535+2205 and 3EG J0534+2200, not reported in the picture.

The black circles represent the other known gamma sources near to the analysed TeV source. In particular, 3EG J0516+2320, 3EG J0520+2556, 3EG J0521+2147 are completely visible, and 3EG J0542+2610 is partially visible on the upper part of the map.

The flux of TeV J0534+220 measured on this OB is

$(204.3 \pm 22.8) \times 10^{-8}$ ph cm^{-2} s^{-1} $(E_\gamma \geq 100$ MeV)

$(36.0 \pm 6.3) \times 10^{-8}$ ph cm^{-2} s^{-1} $(E_\gamma \geq 400$ MeV)

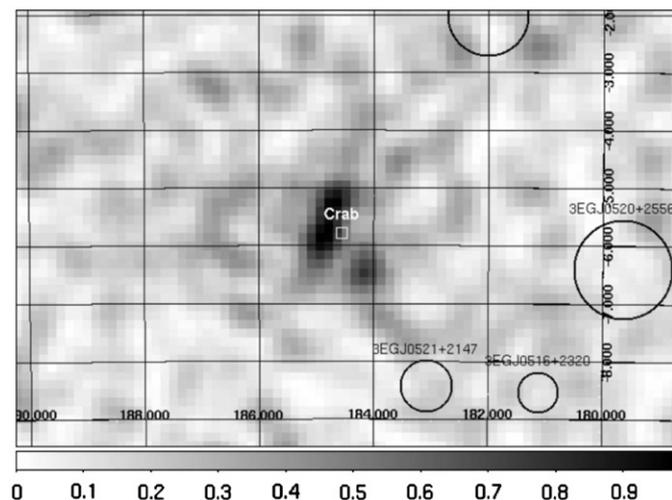**Fig. 3.** Counts map of the source TeV J0534+220 (identified as *Crab*), located at $l = 184.56°$, $b = -5.78°$, with energy threshold $E_\gamma \geq 100$ MeV. The black circles represent the known gamma sources near to the analysed TeV source.
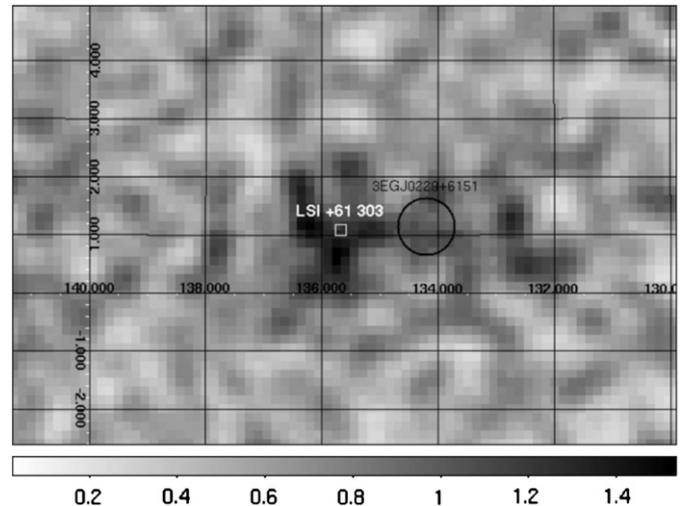

Fig. 4. Counts map of the source TeV J0240+611 (identified as *LSI +61 303*), located at $l = 184.56°$, $b = -5.78°$, with energy threshold $E_\gamma \geq 100$ MeV. The black circle represents the known gamma source 3EG J0229+6151 near to the analysed TeV source.

fully compatible with the following result published on the *First AGILE Catalog of High Confidence Gamma-Ray Sources* [9]

$(220 \pm 15) \times 10^{-8}$ ph cm^{-2} s^{-1} $(E_\gamma \geq 100$ MeV)

4.2. LSI +61 303

This source, reported on the TeVCat catalog with the name TeV J0240+611, is located at $l = 184.56°$, $b = -5.78°$. This position corresponds to the known gamma sources 0FGL J0240.3+6113, 1AGL J0242+6111 and 1AGL J0242+6111.

Fig. 4 shows the count map relative to the OB from 2009-01-19 18:00 (UT) to 2009-02-28 12:00 (UT), with an energy threshold of 100 MeV. The measured flux in this period is

$(40.1 \pm 8.6) \times 10^{-8}$ ph cm^{-2} s^{-1} $(E_\gamma \geq 100$ MeV)

$(4.9 \pm 1.8) \times 10^{-8}$ ph cm^{-2} s^{-1} $(E_\gamma \geq 400$ MeV)

that is in good agreement with the correspondent value

$(54 \pm 12) \times 10^{-8}$ ph cm^{-2} s^{-1} $(E_\gamma \geq 100$ MeV)

published on the First AGILE catalog.

4.3. Markarian 421

This source, located at $l = 179.8°$, $b = 65.0°$, is reported on the TeVCat catalog as TeV J1104+381 and has correspondence with the known gamma sources 0FGL J1104.5+3811, 1AGL J1104+3754 and 3EG J1104+3809.

Since this source, shown in Fig. 5, is quite far from the galactic plane, the exposure accumulated by AGILE GRID in this region is rather low, and the flux calculation allows to obtain only the upper limit for all of the 5 OBs in which the source was visible.

The flux upper limit computed for the OB starting on 2008-06-09 18:00 (UT) and ending on 2008-06-15 12:00 (UT) is

$(34.6 \pm 16.0) \times 10^{-8}$ ph cm^{-2} s^{-1} $(E_\gamma \geq 100$ MeV)

This is comparable with the more accurate value specifically computed with a most detailed procedure when an evident Mkn 421 flare occurred in June 2008. In the published results [12] the measured flux resulted from an integration over the whole 5-day period (~ 260 ks) from 2008-06-09 17:02 (UT) to 2008-06-15
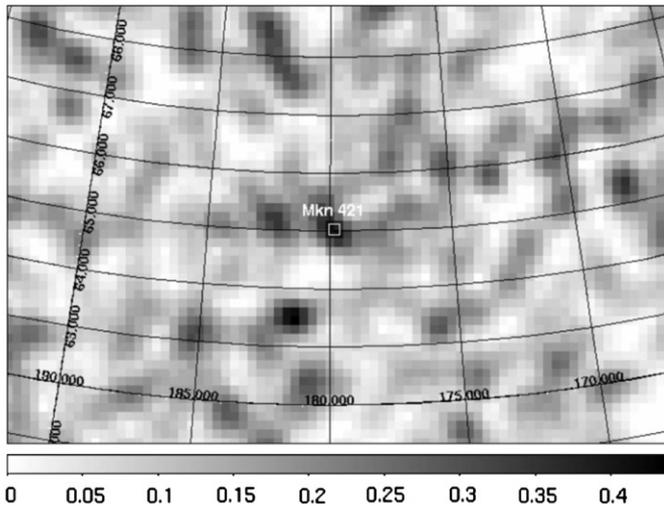
Fig. 5. Counts map of the source TeV J1104+381 (identified as *Markarian 421*), located at $l = 179.8°$, $b = 65.0°$, with energy threshold $E_\gamma \geq 100$ MeV.

02:17 (UT) is

$$(42^{+14}_{-12}) \times 10^{-8} \, \mathrm{ph \, cm^{-2} \, s^{-1}} \quad (100 \, \mathrm{MeV} \geq E_\gamma \geq 10 \, \mathrm{GeV})$$

5. Conclusions and discussion

The automatic analysis performed on the known TeV sources using the AGILE GRID data collected during the first two years of operation has produced some meaningful preliminary results, that can be compared with the *First AGILE Catalog of High Confidence Gamma-Ray Sources* results and with those obtained by the other VHE experiments.

The used automatic procedure allowed to extract the flux values for 73 sources—both galactic and extragalactic—in several different time periods, and with different energy thresholds.

In some case the automatic detection needs to be improved, applying a dedicated and more specific control on defining the conditions due to the presence of other gamma sources in the region of interest.

These results and the analysis procedure will be the subject of a forthcoming paper, and will be the basis of a detailed study of the TeV sources in the GeV energy range.

In the following paper we will analyze in more detail both the flux values and the source location of the tentative GeV counterparts of the TeV sources, since at present only few common sources are found in terms of positional coincidence and spectral consistency [13].

Acknowledgements

References

[1] M. Tavani, et al., Nucl. Instr. and Meth. A 588 (2008) 52.
[2] F. Perotti, et al., Nucl. Instr. and Meth. A 556 (2006) 228.
[3] M. Prest, et al., Nucl. Instr. and Meth. A 501 (2003) 280.
[4] M. Feroci, et al., Nucl. Instr. and Meth. A 581 (2007) 728.
[5] C. Labanti, et al., Nucl. Instr. and Meth. A 598 (2009) 470.
[6] ⟨http://tevcat.uchicago.edu⟩.
[7] T.C. Weekes, in: High Energy Gamma Ray Astronomy, Proceedings of the 4th International Meeting on High Energy Gamma-Ray Astronomy, AIP Conference Proceedings, vol. 1085, 2008, p. 3.
[8] R.C. Hartman, et al., ApJS 123 (1999) 79.
[9] C. Pittori, et al., A&A 506 (2009) 1563.
[10] A.A. Abdo, et al., ApJS 183 (2009) 46.
[11] S.S. Wilks, Ann. Math. Statist. 9 (1938) 60.
[12] I. Donnarumma, ApJ 691 (2009) L13.
[13] S. Funk, et al., ApJ 679 (2008) 1299.